2-6-2004

Ca2+ syntillas, miniature Ca2+ release events in terminals of hypothalamic neurons, are increased in frequency by depolarization in the absence of Ca2+ influx

Valerie De Crescenzo
University of Massachusetts Medical School

Ronghua ZhuGe
University of Massachusetts Medical School

Cristina M. Velazquez-Marrero
University of Massachusetts Medical School

See next page for additional authors

Ca2+ syntillas, miniature Ca2+ release events in terminals of hypothalamic neurons, are increased in frequency by depolarization in the absence of Ca2+ influx

Authors
Valerie De Crescenzo, Ronghua ZhuGe, Cristina M. Velazquez-Marrero, Lawrence M. Lifshitz, Edward E. Custer, Jeffrey Carmichael, F. Anthony Lai, Richard A. Tuft, Kevin E. Fogarty, Jose R. Lemos, and John V. Walsh

Comments
Co-author Cristina M. Velazquez-Marrero is a student in the Neuroscience program in the Graduate School of Biomedical Sciences (GSBS) at UMass Medical School.

Cellular/Molecular

Ca^{2+} Syntillas, Miniature Ca^{2+} Release Events in Terminals of Hypothalamic Neurons, Are Increased in Frequency by Depolarization in the Absence of Ca^{2+} Influx

Valérie De Crescenzo,[1] Ronghua ZhuGe,[1,2] Cristina Velázquez-Marrero,[1] Lawrence M. Lifshitz,[1,2] Edward Custer,[1] Jeffrey Carmichael,[2] F. Anthony Lai,[3] Richard A. Tuft,[1,2] Kevin E. Fogarty,[1,2] José R. Lemos,[1] and John V. Walsh Jr[1]

[1]Department of Physiology, University of Massachusetts Medical School, Worcester, Massachusetts 01655, [2]Biomedical Imaging Group, University of Massachusetts Medical School, Worcester, Massachusetts 01605, and [3] Wales Heart Research Institute, University of Wales College of Medicine, Cardiff CF14 4XN, United Kingdom

Localized, brief Ca^{2+} transients (Ca^{2+} syntillas) caused by release from intracellular stores were found in isolated nerve terminals from magnocellular hypothalamic neurons and examined quantitatively using a signal mass approach to Ca^{2+} imaging. Ca^{2+} syntillas (*scintilla*, *L.*, spark, from a synaptic structure, a nerve terminal) are caused by release of ~250,000 Ca ions on average by a Ca^{2+} flux lasting on the order of tens of milliseconds and occur spontaneously at a membrane potential of −80 mV. Syntillas are unaffected by removal of extracellular Ca^{2+}, are mediated by ryanodine receptors (RyRs) and are increased in frequency, in the absence of extracellular Ca^{2+}, by physiological levels of depolarization. This represents the first direct demonstration of mobilization of Ca^{2+} from intracellular stores in neurons by depolarization without Ca^{2+} influx. The regulation of syntillas by depolarization provides a new link between neuronal activity and cytosolic [Ca^{2+}] in nerve terminals.

Key words: **calcium imaging; calcium spark; intracellular calcium; neurosecretion; presynaptic; ryanodine receptor**

Introduction

From the time that the central role of Ca^{2+} in neurotransmitter release was first recognized, the study of nerve terminal function and exocytosis has focused intensively on Ca^{2+} influx (Berridge, 1998). In contrast, Ca^{2+} release from internal stores in nerve terminals has received less attention, and its role is controversial (Meldolesi, 2001; Carter et al., 2002). A major problem in this field is that release of Ca^{2+} from presynaptic stores has often been inferred from effects on postsynaptic currents rather than examined directly. Nevertheless, a number of studies using this indirect approach have proved highly informative (Melamed-Book et al., 1999; Llano et al., 2000; Emptage et al., 2001). In addition, direct examination of global changes in neuronal cytosolic [Ca^{2+}] have shown release from intracellular stores via a calcium-induced Ca^{2+} release (CICR) mechanism after Ca^{2+} influx (Narita et al., 1998; Krizaj et al., 1999), but there has been no demonstration of a mechanism wherein depolarization, in the absence of Ca^{2+} influx, causes Ca^{2+} release from stores in terminals or in any other neuronal structure.

The direct observation and analysis of miniature Ca^{2+} release events in non-neuronal cells has contributed greatly to our understanding of the role and regulation of Ca^{2+} stores (Bers, 2002). These miniature events were first observed in response to IP_3 in oocytes and designated "Ca^{2+} puffs" by Parker and Yao (1991) and then found in myocytes, where they were mediated by ryanodine receptors (RyRs) and designated "Ca^{2+} sparks" (Cheng et al., 1993). Ca^{2+} transients, resembling puffs and sparks in some respects, have been observed in cultured hippocampal preparations (Koizumi et al., 1999), and three recent studies have provided indications of spontaneous transients in nerve terminals. First, Melamed-Book et al. (1999) found outliers in the fluorescence noise of Ca^{2+} images in cultured hippocampal somata and neuron terminals at the lizard neuromuscular junction, which they compared to spontaneous Ca^{2+} sparks in muscle. Importantly, in the cell bodies of hippocampal cultures, Melamed-Book et al. (1999) observed the noise outliers in Ca^{2+}-free medium, whereas in the nerve terminals the Ca^{2+} transients were not studied in Ca^{2+}-free medium, leaving their intracellular origin in doubt. Second, Llano et al. (2000) in their landmark study on "maximinis" observed long duration Ca^{2+} transients lasting seconds in presumed nerve terminals. Third, Emptage et al. (2001) illustrated several instances of spontaneous Ca^{2+} transients in axon-like processes and synaptic boutons. However, neither of these latter two studies demonstrated spontaneous transients in Ca^{2+}-free medium or blockade by ryanodine (see Discussion). Moreover in none of the preceding studies were the effects of membrane potential on the observed Ca^{2+} transients examined.

Received Sept. 20, 2003; revised Dec. 9, 2003; accepted Dec. 11, 2003.

This work was supported by grants from the National Institutes of Health (HL61297 to J.W., DA10487 to J.L.), and a Wellcome Trust grant to F.A.L. We thank Stephen Baker for assistance with statistical analysis of data and Tom Knott for experimental advice.

Correspondence should be addressed to John V. Walsh, Department of Physiology, University of Massachusetts Medical School, Worcester, MA 01655. E-mail: John.Walsh@umassmed.edu.

DOI:10.1523/JNEUROSCI.4286-03.2004

 0270-6474/04/241226-10$15.00/0

In the present study we observed spontaneous, miniature, highly localized, short-lived Ca^{2+} transients, which arise from intracellular Ca^{2+} stores in single isolated nerve terminals from hypothalamic neurons. Because they resemble Ca^{2+} sparks in muscle in some, but not all respects, they were designated Ca^{2+} syntillas (*scintilla*, *L.*, spark, from a synaptic structure, a nerve terminal). We also quantified the transients by using the same signal mass approach previously used in studies of Ca^{2+} sparks (ZhuGe et al., 1999, 2000, 2002). Surprisingly, physiological levels of depolarization, in the absence of Ca^{2+} influx, increased syntilla frequency without significant effect on the amplitude of individual syntillas. To the best of our knowledge, this is the first direct demonstration of release of Ca^{2+} from intraneuronal stores elicited by depolarization in the absence Ca^{2+} influx. By virtue of their regulation by membrane potential, Ca^{2+} syntillas provide a new functional link between neuronal activity and cytosolic [Ca^{2+}] in nerve terminals. A preliminary report of this work has been published previously (De Crescenzo et al., 2003).

Materials and Methods

Whole-terminal patching

Tight-seal, "whole terminal" recording on nerve terminals (Lemos and Nowycky, 1989) freshly prepared from adult Swiss Webster mice (Nordmann et al., 1987) was done with an Axopatch-1D amplifier. Pipette solution (in mM): 0.05 K_5fluo-3 (Molecular Probes, Eugene, OR), 135 KCl, 2 $MgCl_2$, 30 HEPES, 4 MgATP, and 0.3 Na-GTP, pH 7.2. Bath solution: 135 NaCl, 5 KCl, 10 HEPES, 10 glucose, 1 $MgCl_2$, and 2.2 $CaCl_2$, pH 7.2. Ca^{2+}-free bath solution: 135 NaCl, 5 KCl, 10 HEPES, 10 glucose, 0.2 EGTA, and 1 $MgCl_2$, pH 7.2. We added 100 μM Ca^{2+} and 100 μM Cd^{2+} to the latter bath solution in the absence of EGTA for experiments with these ions. To prevent depletion of Ca^{2+} from internal stores, the terminals remained in normal Locke's solution (2.2 mM Ca^{2+}) until the beginning of the experiment, and the duration of the Ca^{2+}-free protocol was ~15 min (ZhuGe et al., 1999). Resting global cytosolic [Ca^{2+}] determined with the ratiometric indicator fura-2 (50 μM in the patch pipette) under the same conditions (but fluo-3 absent) was performed according to the method of Grynkiewicz et al. (1985) with an assumed Ca^{2+}-fura 2 K_D of 200 nM, as previously described (Becker et al., 1989). Resting values for global cytosolic [Ca^{2+}] in the presence and absence of extracellular Ca^{2+} were 68.5 ± 22.3 nM ($n = 7$) and 46.2 ± 7.5 nM ($n = 8$), respectively, and these values were not significantly different ($p = 0.4$). These values agree well with previous estimates in these terminals (Troadec et al., 1998). Reagents (from Sigma, St. Louis, MO, unless otherwise noted) were bath perfused or delivered by a " picospritzer" (Parker, Hollis, NH). In the latter case, 170 ± 36 msec ($n = 5$) was required for the solution to reach the nerve terminal, and an additional 426 ± 126 msec to reach an equilibrium around the terminal, as determined by a "puff" of 100 mM KCl (replacing NaCl) to induce an inward current. Terminals were suspended from tip of the patch pipette out of contact with the floor of the chamber.

Image acquisition and data analysis

General. Fluorescence images using fluo-3 as a calcium indicator were obtained using a custom-built wide-field digital imaging system (ZhuGe et al., 1999). Rapid imaging at 200 Hz (exposure, 5 msec) or 50 Hz (exposure, 10 msec) was made possible by equipping the system with a cooled high-sensitivity, charge-coupled device camera developed in conjunction with the Massachusetts Institute of Technology Lincoln Laboratory (Lexington, MA) (ZhuGe et al., 1999) (Fig. 1). The camera was interfaced to a custom-made inverted microscope. The terminals were imaged using a 100× Nikon 1.4 NA oil immersion objective, giving a pixel size of 133 nm at the specimen. A laser shutter controlled the exposure duration. The 488 nm line of an argon–ion laser (Coherent) provided fluorescence excitation, and emission of the Ca^{2+} indicator was monitored at wavelengths >500 nm. Subsequent image processing and analysis was performed off-line using a custom-designed software package, running on either a Silicon Graphics or Linux/PC workstation. Two quantitative measures of Ca^{2+} were used: one to assess the properties of transient, focal increases in Ca^{2+}, i.e., Ca^{2+} syntillas, and another to asses global increases in Ca^{2+}.

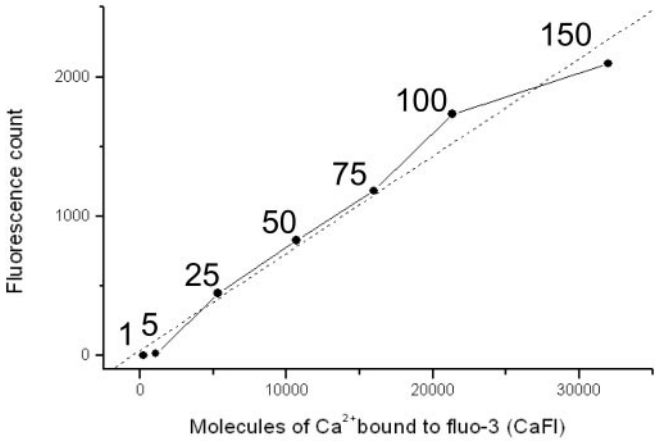

Figure 1. Relationship between measured fluorescence and amount of Ca^{2+} bound to fluo-3 (CaFl). To determine the total amount of Ca^{2+} released in a syntilla (Ca_T), measured fluorescence was determined as a function of the amount of Ca^{2+} bound to fluo-3 (CaFl). Images were acquired of glass capillaries (internal rectangular cross section 20-μm-deep and 200-μm-wide) loaded with known concentrations of fluo-3 (1, 5, 25 50, 75, 100, and 150 μM for each of the points shown from left to right along the abscissa) and saturating [Ca^{2+}] (1.45 mM). Data were fitted with a straight line ($r = 0.85$) having a slope of 0.072 intensity units per fluo-3 molecule per msec exposure (14 molecules of bound fluo-3 per count per millisecond).

Signal mass. To assess the properties of Ca^{2+} syntillas and do so quantitatively, the signal mass approach was used, as conceptualized by Sun et al. (1998) and developed for analysis of Ca^{2+} sparks using wide-field microscopy by ZhuGe et al. (2000). A brief summary of the signal mass method, which is described in detail in ZhuGe et al. (2000) follows. During a syntilla, free Ca^{2+} (diffusion coefficient, $D = 250$ μm^2/sec) and Ca^{2+} bound to fluo-3 ($D = 22$ μm^2/sec) (Smith et al., 1998) quickly diffuse in three dimensions away from the release site as Ca^{2+} continues to be discharged. Therefore, to quantify the increase in total fluorescence, i.e., the Ca^{2+} signal mass (ΔCaFl) resulting from the binding of fluo-3 to the discharged Ca^{2+}, fluorescence must be collected from a sufficiently large volume surrounding the release site. The optimal value for this volume was found to be that subtended by an area of 116 μm^2 (81 × 81 pixels). Because photons must be collected from a three-dimensional (3-D) volume and not simply from a single plane, wide-field microscopy is well suited to this method.

To relate the measured increase in fluorescence to the total amount of Ca^{2+} released in a single syntilla (Ca_T), a calibration curve was constructed that related measured fluorescence to the amount of Ca^{2+} bound to fluo-3 (ΔCaFl) (O'Reilly et al., 2003). The same illumination conditions, optical pathway, and CCD camera configuration were used as in measurements on the terminals. Glass capillaries (Vitro Dynamics, Rockaway, NJ), with an internal rectangular cross section 20-μm-deep by 200-μm-wide, were loaded with solutions containing known concentrations of fluo-3 (Fig. 1), saturating [Ca^{2+}] (total [Ca^{2+}] = 2.2 mM and free [Ca^{2+}] = 1.45 mM), and otherwise the same intracellular solutions used to load the patch pipette. The capillaries were placed on the microscope stage and imaged with the CCD camera using 1 msec exposures. The total fluorescence intensity (TFI) at each concentration was measured by summing the light from over an area of 127 × 128 pixels, equivalent to 287.55 μm^2. Because this is wide-field microscopy, the entire depth of the capillary is illuminated, and all photons, both in-focus and out-of-focus from the entire thickness of the capillary are collected. The total number of fluo-3 molecules was calculated by multiplying the [fluo-3] by the total imaged volume of 287.55 × 20, or 5751 $\mu m^{3.}$ When the TFI data were plotted against the corresponding total number of molecules, the relationship was linear over a wide range of [fluo-3] up to 100 μM. The data were fit with a straight line ($r = 0.99$) having a slope of 0.072 intensity units per molecule of fluo-3 in 1 msec (Fig. 1). Thus, for

example, each intensity unit measured in a 5 msec imaging period corresponds to ~2.79 molecules of Ca^{2+} bound to fluo-3.

Because "whole-terminal" patch recording was used at the same time that images were acquired, endogenous mobile buffers were presumably dialyzed away, and so can be neglected. In the absence of all other buffers, 50 μM fluo-3 binds >97% of Ca^{2+} entering the cytosol for Ca^{2+} currents ranging from 0.1–10 pA (ZhuGe et al., 2000). Such a Ca^{2+} current entering the cytosol from intracellular stores in the case of a syntilla is designated as $I_{Ca(syntilla)}$. Thus, the peak signal mass provides a faithful indicator of Ca_T in the absence of buffers other than fluo-3. However, endogenous non-mobile buffers alter the magnitude and time course of the signal mass and hence determinations of Ca_T and $I_{Ca(syntilla)}$; these effects can be dealt with as follows. The binding ratio (κ) of a buffer (Zhou and Neher, 1993) at equilibrium is: $\kappa = \delta[CaB]/\delta[Ca]$. Ca_T, the total amount of Ca^{2+} released in a single syntilla, is: $Ca_T = (\Delta[CaFl] + \Delta[Ca^{2+}] + \Delta[CaBuf]) \times$ Volume, with [CaFl] the concentration of Ca^{2+} bound to fluo-3, $[Ca^{2+}]$ the concentration of free Ca^{2+}, and [CaBuf] the concentration of Ca^{2+} bound to endogenous non-mobile buffers. Noting that $\Delta[CaFl] = \kappa_{fluo\text{-}3}\,\Delta[Ca^{2+}]$ and $\Delta[CaBuf] = \kappa_{buf}\,\Delta[Ca^{2+}]$, then $Ca_T = \Delta CaFl\,(1 + 1/\kappa_{fluo\text{-}3} + \kappa_{buf}/\kappa_{fluo\text{-}3})$, where $\kappa = [B_T] \times K_D/([Ca^{2+}] + K_D)^2$, with $[B_T]$ total concentration of a buffer and K_D its dissociation constant. For free $[Ca^{2+}]_i$ of 46.2 nM (in the case of the Ca^{2+}-free extracellular solution; see above) or 68.5 nM (in the case of the extracellular solution containing normal $[Ca^{2+}]$; see above), $\kappa_{fluo\text{-}3}$ had values of 41.0 and 39.5, respectively, and κ_{buf} was previously determined as 174 in the rat for small global increases (<100 nM) in $[Ca^{2+}]$ (Stuenkel, 1994). Therefore $Ca_T = 5.27 \times \Delta CaFl$ or $5.43 \times \Delta CaFl$ at equilibrium, for the Ca^{2+}-free and normal $[Ca^{2+}]$ extracellular solutions, respectively. These expressions are used to calculate signal mass in all figures. However, because the estimate of Ca_T from $\Delta CaFl$ assumes equilibrium, determination of $I_{Ca(syntilla)}$ by differentiating the signal mass trace during its rising phase (when equilibrium may not obtain) is not accurate. Using the derivative of the signal mass trace to estimate the underlying $I_{Ca(syntilla)}$ requires the rate constants of the endogenous buffers that are presently unknown. Hence, the determination of $I_{Ca(syntilla)}$ in Figure 4 is uncorrected for the effects of endogenous buffers, and therefore its peak value is a low estimate.

Metric for global $[Ca^{2+}]_i$ and images

For a measure of global increases in $[Ca^{2+}]_i$ using fluo-3, the conventional fluorescence ratio, $\Delta F/F_0$, measured over the entire terminal was used as described previously (Cannell et al., 1995). Finally, the fluorescence in the images shown is also computed as $\Delta F/F_0$ for each pixel.

In all cases, data are reported as mean ± SEM; n is the number of syntillas, and N is the number of observations. Statistical analysis of difference was made with Mann–Whitney U test, and the p values have been Bonferroni adjusted, as appropriate, with $p < 0.05$ considered significant.

Simulations of the spatiotemporal profile of $[Ca^{2+}]$ arising from a syntilla

To gain insight into the possible role of syntillas, we modeled a terminal and simulated syntillas, and examined the spatial and temporal profile of free $[Ca^{2+}]$ that resulted at the plasma membrane where vesicle fusion would occur. Finite difference approximations were used to solve a set of partial differential equations for the reaction–diffusion kinetics in a cylindrical coordinate system. The details of this approach are described elsewhere (Kargacin and Fay, 1991), and it has been used before for analyzing the spatiotemporal profile of $[Ca^{2+}]$ resulting from Ca^{2+} sparks in smooth muscle (ZhuGe et al., 2000, 2002). The terminal was modeled as a cylinder, 6 μm in diameter and 3 μm in height. The Ca^{2+} release site was modeled as a small cylinder, 100 nm in diameter and height, located either directly under the plasma membrane (PM) as shown in the diagram on the right side of Figure 7*B* or 400 nm inward from the PM as shown in Figure 7*C*. The simulation included:1.676 mM of fixed (non-diffusible) buffer, $K_d = 10$ μM, $k_{on} = 5 \times 10^5$ mM^{-1} S^{-1}, $k_{off} = 5 \times 10^3$ S^{-1}, and 100 μM of a (slowly) diffusible buffer, $K_d = 10$ μM, $k_{on} = 5 \times 10^5$ mM^{-1} S^{-1}, $k_{off} = 5 \times 10^3$ S^{-1}, $D = 1.5 \times 10^{-7}$ cm^2 S^{-1}. The total concentration of fixed and slowly diffusible buffers were derived from the buffering capacity determined by Stuenkel (1994) for these terminals. Because detailed information about the kinetics of the buffers in these terminals is not available, the on and off kinetics were taken to be the same as those determined by Klingauf and Neher (1997) in another neuroendocrine cell, the bovine adrenal chromaffin cell.

Immunocytochemistry

Nerve terminals, isolated as described above and plated onto poly-L-lysine-coated coverslips were placed in 2% paraformaldehyde (PFA) in PBS at pH 7.5, which was then raised to 10 to increase efficacy of the fixation. Terminals were then permeabilized (0.1 M ethanolamine in PBS plus 0.1% Triton X-100, pH 8) and washed with PBS to be immunolabeled. Antibody (Ab) buffer solution consisted of 2% BSA, 2% donkey serum, and 200 μg/ml normal donkey IgG in PBS, pH 7.7. A rabbit polyclonal antiserum was raised to the C-terminal sequence of 16 amino acids that is 100% conserved in all known mammalian RyRs (Tunwell et al., 1996). Terminals were incubated for 1 hr in the presence of secondary Abs, and then post-fixed in 2% PFA–PBS. 3-D fluorescence imaging was performed on an inverted wide-field microscope (Nikon Diaphot 200). Terminals were excited with a 100 W mercury lamp. Images were obtained through a 60× objective and digitally recorded on a cooled, back-thinned CDD camera (Photometrics, Tucson, AZ) with an effective pixel size at the specimen of 83 nm in x–y and a z spacing of 250 nm. This results in a 3-D stack of ~25 images planes of each terminal (Carrington et al., 1995). Two sets of controls consisting of either preimmune serum or secondary antibodies were both significantly dimmer than the terminals incubated with the specific antiserum. Terminals that stained positive for RyRs also stained positive for either AVP or oxytocin neurophysin (data not shown).

Results

We used a preparation of freshly dissociated mouse nerve terminals (Nordmann et al., 1987) from hypothalamic neurons, which for the most part terminate in the posterior pituitary (Burbach et al., 2001). The data were drawn from experiments on >179 terminals. As has been pointed out previously (Wang et al., 1993; Neher, 1998), these terminals are ideally suited for detailed functional studies for a number of reasons. First, they can be immediately studied after isolation, so that changes that may occur in culture are avoided; and second, they are large enough to be patched in "whole-terminal" mode (Lemos and Nowycky, 1989). The latter allowed us to control the membrane potential and to load the fluorescent Ca^{2+} indicator, fluo-3 (50 μM), through the pipette in the salt form. This form of loading, unlike the AM derivative form, ensures that the indicator is localized to the cytosol and that the concentration of indicator is the same in each terminal, which is critical if quantitative interterminal comparisons are to be made. Imaging was performed with a high-speed, wide-field digital imaging system (as opposed to a confocal system), developed in collaboration with MIT Lincoln Laboratory (ZhuGe et al., 1999).

Spontaneous Ca^{2+} syntillas arise from intraterminal stores

When the nerve terminals were held at a membrane potential of −80 mV in the absence of extracellular Ca^{2+} (0 Ca^{2+} together with either 200 μM or 1 mM extracellular EGTA), we observed Ca^{2+} syntillas, spontaneous, brief, miniature Ca^{2+} transients of the type illustrated in Figure 2, *A* and *B* (see supplementary material for movie, available at www.jneurosci.org). The Ca^{2+}-free condition establishes the intracellular origin of the Ca^{2+} responsible for the syntillas. In these and subsequent experiments, the exposure of the terminals to a Ca^{2+}-free environment was kept to a minimum, as described in Materials and Methods, to avoid depletion of the intracellular stores. Ca^{2+} syntillas were also observed at −80 mV in the presence of normal extracellular $[Ca^{2+}]$ (Fig. 2*D*) and also in the presence of both extracellular Ca^{2+} (100 μM) and Cd^{2+}, the latter applied by puffer pipette (200 μM). At

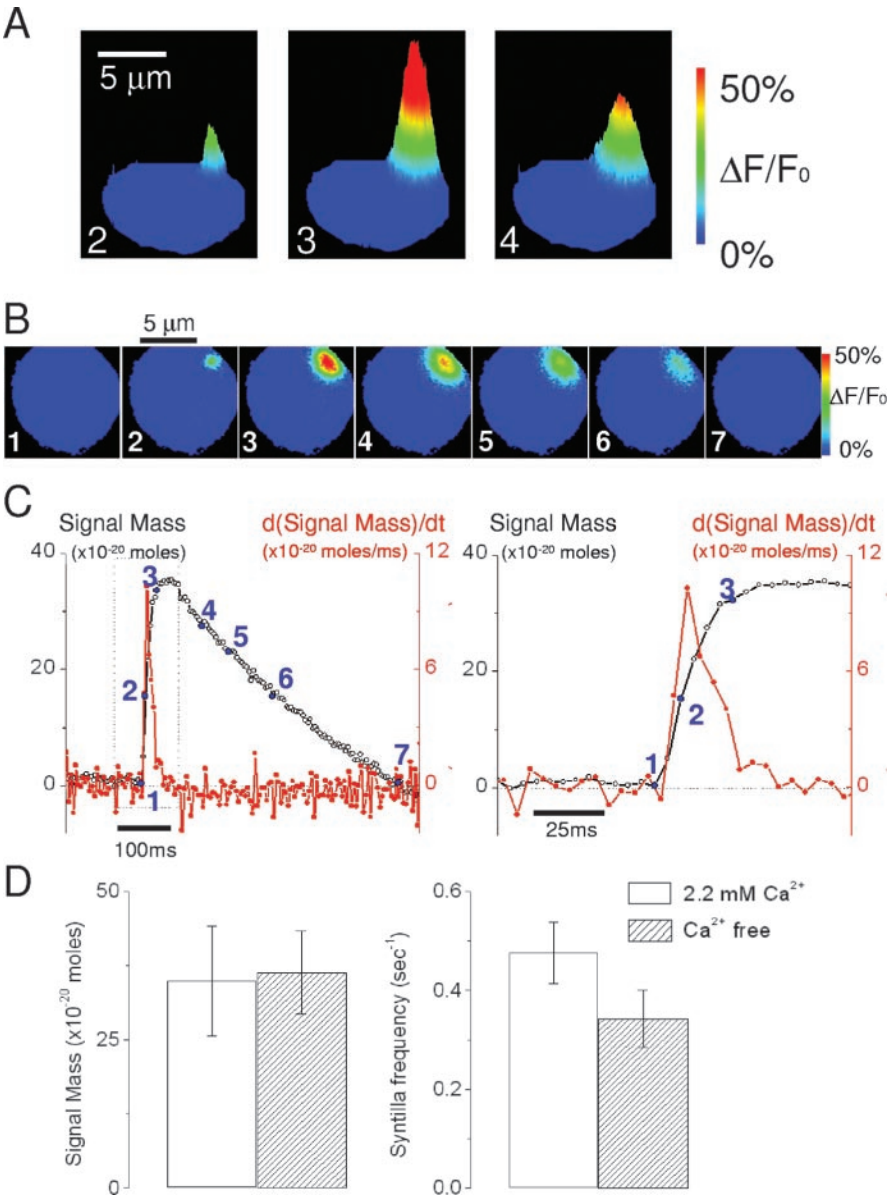

Figure 2. Spontaneous Ca^{2+} syntillas in isolated nerve terminals in Ca^{2+}-free solution at a membrane potential of −80 mV. *A*, *B*, Images of one Ca^{2+} syntilla in a single isolated terminal in Ca^{2+}-free solution (200 μM EGTA) at a holding membrane potential, $V_h = -80$ mV. Contour plots (*A*) show same syntilla as *B*. *C*, Time course, corresponding to the images in *A* and *B*, of signal mass (black) and its first derivative (red); expanded time scale on right. *D*, Neither syntilla frequency ($N = 13$ and 18, with and without Ca^{2+}, respectively) nor Ca^{2+} signal mass ($n = 22$ and 27, with and without Ca^{2+}, respectively) were altered by extracellular calcium at $V_h = -80$ mV. *N* represents the number of observation periods for 21 nerve terminals used, and *n* represents the number of syntillas.

−80 mV we saw no instances of Ca^{2+} waves spreading over the terminal; hence, in no case did Ca^{2+} syntillas trigger Ca^{2+} waves.

The magnitude of each individual syntilla was characterized by its signal mass, a measure devised by Sun et al. (1998) and developed for wide-field imaging in earlier work of ours (ZhuGe et al., 2000). The Ca^{2+} signal mass (ΔCaFl) is the total increase in fluorescence caused by the Ca^{2+} that binds to fluo-3 after entering the cytosol, from internal stores in the present instance (Fig. 2*C*). Because Ca^{2+} and bound fluo-3 rapidly diffuse away from the syntilla release site, the increase in fluorescence was collected from a sufficiently large volume in the region of the syntilla to capture fluorescence caused by all the Ca^{2+} released (ZhuGe et al., 2000) (see Materials and Methods). Thus, at its plateau the Ca^{2+} signal mass is directly proportional to the total amount of Ca^{2+} released into the cytosol in a single syntilla (Ca_T), as given by: $Ca_T = \Delta CaFl\ (1 + 1/\kappa_{fluo\text{-}3} + \kappa_{buf}/\kappa_{fluo\text{-}3})$, where ΔCaFl is the increase in amount of Ca^{2+} bound to fluo-3, and κ_{buf} and $\kappa_{fluo\text{-}3}$ are the "binding ratios" (Naraghi and Neher, 1997) of fluo-3 and non-mobile endogenous buffers (Stuenkel, 1994), respectively, as defined in Materials and Methods. Hence, the signal mass is given in moles of Ca^{2+} (Fig. 2*C*), as calculated in Materials and Methods. Because the signal mass is not a measure of Ca^{2+} concentration ($[Ca^{2+}]_i$) but an integrated signal giving Ca_T (Fig. 2*C*, black lines), its derivative (Fig. 2*C*, red lines) is a function of the underlying Ca^{2+} current ($I_{Ca(syntilla)}$) entering the cytosol from internal stores. (The ability to determine Ca_T depends on the assumption of negligible removal of Ca^{2+} from the cytosol before the peak of the signal mass; this appears justified because the rise of the signal mass is considerably faster than its decay and because $[Ca^{2+}]_i$ is high only in a small region for a short time).

If syntillas arise solely from intracellular stores, they should not differ in the presence or absence of extracellular Ca^{2+}. This was in fact the case. Spontaneous Ca^{2+} syntillas at a holding potential (V_h) of −80 mV had the same frequency and the same Ca^{2+} signal mass in the presence of extracellular Ca^{2+} as in its absence (Fig. 2*D*). Because the signal mass of each syntilla at its plateau (Fig. 2*C*) is directly proportional to the total Ca^{2+} released and hence to the product of the mean $I_{Ca(syntilla)}$ and its duration, it is unlikely that either changed substantially in the presence or absence of external Ca^{2+}; otherwise the change in the magnitude of $I_{Ca(syntilla)}$ must compensate exactly for the change in its duration.

Ca^{2+} syntillas are mediated by RyRs

Four lines of evidence indicated that syntillas are mediated by RyRs. First, ryanodine, a blocker of RyRs at the concentration used (100 μM in the bathing solution) (ZhuGe et al., 1999; Llano et al., 2000), decreased spontaneous syntilla frequency, but did not alter the total amount of Ca^{2+} released by an individual syntilla (Fig. 3*A*) (see Discussion). Second, brief (4 sec) applications of caffeine, which increases the probability of RyR opening and inhibits IP_3 receptors (Ehrlich et al., 1994), increased both syntilla frequency and the total Ca^{2+} released by an individual syntilla (see Discussion). Furthermore, ryanodine blocked this increase in frequency, again without affecting the total Ca^{2+} released by an individual syntilla (Fig. 3*A*). Third, ryanodine at a lower concentration (10 μM in the puffer pipette) increased syntilla frequency, similar to the increase in Ca^{2+} spark frequency

seen in striated muscle (Gonzalez et al., 2000; Hui et al., 2001), whereas it decreased the total amount of Ca^{2+} released by an individual syntilla (Fig. 3*B*) (see Discussion). Fourth, RyRs were identified immunocytochemically in the terminals, and they were not confined to one region of the terminal (Fig. 3*C*). However, the RyRs were not uniformly distributed throughout the terminal but had a somewhat higher density near the periphery, as is evident from the stereo pair in Figure 3*C*. Similarly, syntilla sites were not confined to one region of the terminal (Fig. 3*D*,*E*). Figure 3*D* shows images of six different syntillas arising from different sites in the same terminal, and Figure 3*E* is a map indicating the site of all the syntillas recorded from that terminal. The right panel of Figure 3*E* indicates the magnitude of each of these syntillas, with the diameter of each circle proportional to the total amount of Ca^{2+} released in that syntilla. Moreover, thapsigargin (TG; 2 μM in the bathing solution) greatly decreased syntilla frequency from 0.31 ± 0.06 ($N = 25$) to 0.05 ± 0.03 ($N = 14$) ($p = 0.004$) in the presence of extracellular Ca^{2+}. (The average amount of Ca^{2+} released per syntilla was 35.23 ± 8.10 × 10^{-20} moles ($n = 29$) in controls versus 40 +/− 21 ($n = 2$), but these values could not be adequately compared because there were so few syntillas in the presence of TG.) The effects of TG indicate that syntilla generation involves a cellular compartment containing SERCA pumps that are generally considered to be confined to the ER. Finally, mitochondria do not appear to be necessary for syntilla generation, because syntillas were still present after 10 min exposure to 2 mM cyanide and 5 mM azide. This treatment was observed to collapse the mitochondrial membrane potential, as measured with a fluorescent probe in parallel experiments (Drummond et al., 2000).

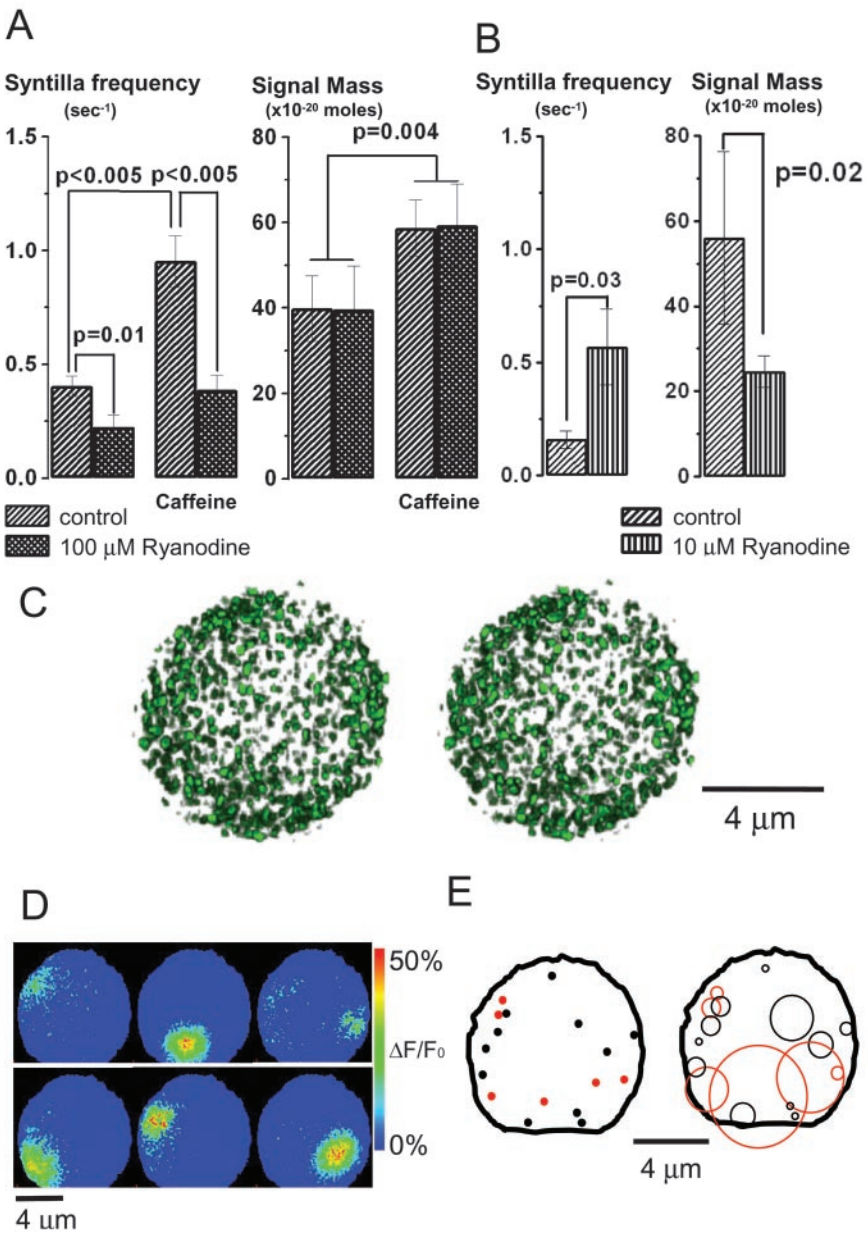

Figure 3. Ca^{2+} syntillas are mediated by RyRs. All experiments were performed in Ca^{2+}-free solution at a membrane potential of −80 mV. *A*, Ryanodine (100 μM in the bathing solution) decreased syntilla frequency ($N = 21$ and 29, without and with ryanodine, respectively) without affecting signal mass ($n = 27$ and 72). Caffeine (20 mM in puffer pipette) increased both frequency ($N = 21$) and signal mass ($n = 55$) at $V_h = -80$ mV, but only the frequency increase was attenuated by ryanodine ($N = 29$) (signal mass data, $n = 19$). *B*, Ryanodine (10 μM in puffer pipette) increased syntilla frequency ($N = 11$) and decreased signal mass ($n = 7$ and 25, without and with ryanodine, respectively). A total of 57 nerve terminals were used for the experiments in *A* and *B*. *C*, RyR receptor localization in a single terminal (stereo pair). A single terminal has been incubated with ryanodine receptor (RyR) antibody and imaged in 3-D. *D*, Images showing six different syntillas in one nerve terminal in Ca^{2+}-free solution, recorded over a period of 8 sec. *E*, Map of locations of all Ca^{2+} syntillas in the same, single terminal illustrated in *D*, recorded over 12 sec ($V_h = -80$ mV). Dots indicate site of one Ca^{2+} syntilla (*E*, left panel); diameters of circles are proportional to the signal mass of the syntilla (*E*, right panel). Red symbols correspond to syntillas in *D*. Recordings in *D* and *E* were made in the presence of 20 mM extracellular caffeine to increase syntilla frequency.

Quantitative characterization of the Ca^{2+} syntilla using the signal mass approach

The signal mass method permits the characterization of the Ca^{2+} syntilla in a quantitative manner. The distribution (Fig. 4*A*) of the total amount of Ca_T per syntilla is exponential with a mean of 40 × 10^{-20} moles of Ca^{2+} or ~250,000 Ca ions released per syntilla. The averaged derivative of signal mass traces (Fig. 4*B*) gives the minimum value for the peak $I_{Ca(syntilla)}$ and the maximal duration of $I_{Ca(syntilla)}$, because buffers act as a filter to decrease the peak and increase the duration of the derivative (see Materials and Methods). Hence, the peak $I_{Ca(syntilla)}$ is at least 1.88 pA on average, and its duration is at most tens of milliseconds. Despite the exponential distribution of Ca_T, $I_{Ca(syntilla)}$ does not appear to be caused by a single RyR channel opening for various durations, because the magnitude of Ca^{2+} current flowing through a single RyR in an artificial bilayer is 0.35 pA (Mejia-Alvarez et al., 1999), considerably smaller than the peak current calculated here (Fig. 4*B*). Thus, it appears that a syntilla

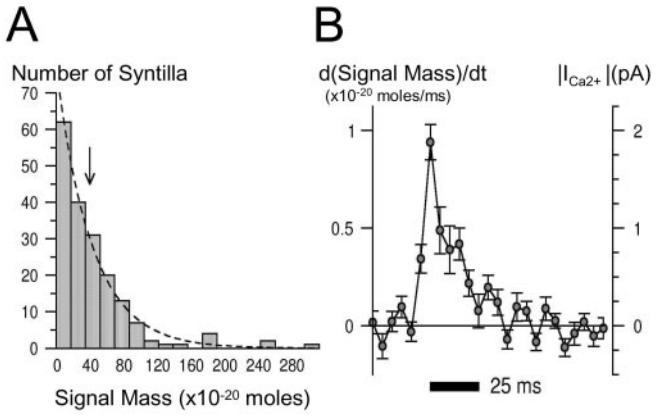

Figure 4. Properties of Ca^{2+} syntillas. (*A*) Distribution of signal mass for 184 Ca^{2+} syntillas from 49 nerve terminals; arrow indicates mean of distribution which is fit by a single exponential ($r^2 = 0.89$). Mean is 43×10^{-20} moles of Ca^{2+} or ~250,000 Ca ions released per syntilla. *B*, Averaged derivative of 17 signal mass traces recorded at a rate of one image per 5 msec. These syntillas were recorded in the presence of a low caffeine concentration (1 mM), which increased their frequency but did not affect the mean signal mass. Calibration of current in *B* does not take account of endogenous buffers (see Materials and Methods).

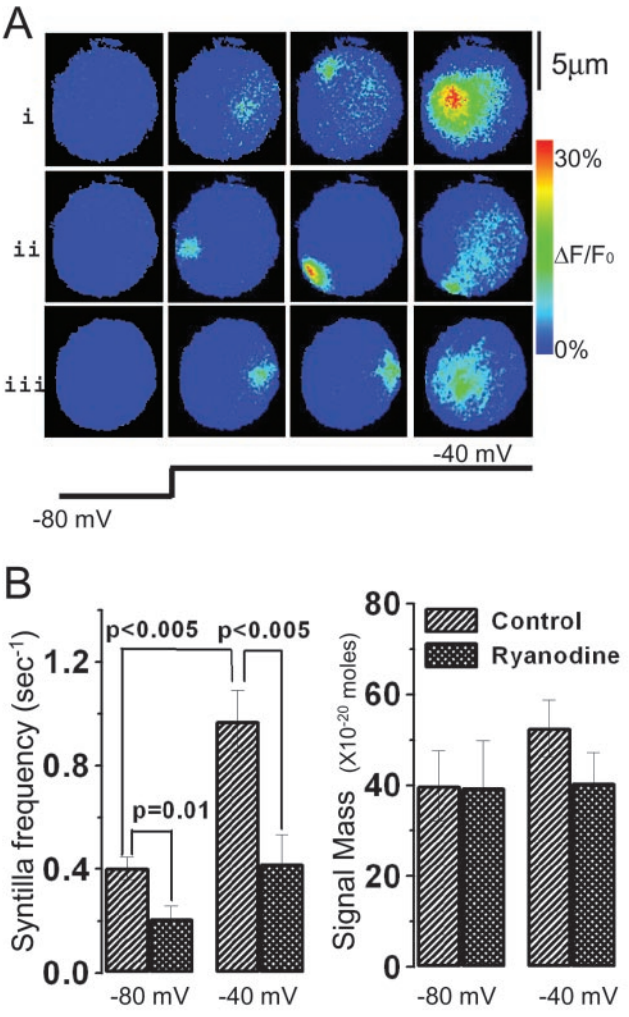

Figure 5. Depolarization from −80 to −40 mV in absence of extracellular Ca^{2+} increases syntilla frequency. Depolarization from −80 to −40 mV elicits two types of response in different terminals: an increase in syntilla frequency (56% of the terminals) (*A*), or an increase in global $[Ca^{2+}]_i$ (44% of the terminals). *A*, Syntillas in a nerve terminal, after depolarization from −80 to −40 mV for 3.8 sec. The terminal was depolarized three times (*i, ii, iii*) with 2 min between depolarizations. *B*, Effect of depolarization from −80 to −40 mV for those terminals in which there was an increase in syntilla frequency ($N = 31$ and 29, at −80 and −40 mV, respectively); there was no change in mean syntilla signal mass ($n = 27$ and 82); ryanodine decreased frequency ($N = 29$ and 28, in the absence and presence of ryanodine, respectively) without affecting signal mass ($n = 40$ and 49). A total of 50 nerve terminals were used for the data in the figure.

does not result from the opening of only one RyR, except perhaps for the smallest syntillas or those below the limit of detection; the same is true for Ca^{2+} sparks in cardiac (Cheng et al., 1993) and smooth muscle (ZhuGe et al., 2000). The spatiotemporal profile of the syntilla is considered below (see Discussion).

Depolarization in the absence of Ca^{2+} influx increases syntilla frequency but does not alter the amount of Ca^{2+} released per syntilla

What regulates syntilla frequency? To investigate the effects of changes in membrane potential without contamination by Ca^{2+} entry, we performed experiments in the absence of extracellular Ca^{2+} (200 μM EGTA). Surprisingly, we found that depolarization from −80 to −40 mV increased syntilla frequency. At −40 mV, two types of responses were observed. In 56% of the terminals, depolarization resulted in an increase in the syntilla rate but not in the signal mass of the individual syntillas (Fig. 5*A*,*B*). Similarly, ryanodine attenuated the increase in frequency without effect on the signal mass (Fig. 5*B*). (In the second type of response, observed in 44% of the terminals, depolarization from −80 to −40 mV caused an increase in global cytosolic $[Ca^{2+}]$. This type of response is considered in the next section.).

Two classes of mechanisms for the increase in syntilla frequency after depolarization in the absence of extracellular Ca^{2+} suggest themselves. The first is a direct voltage-coupling mechanism, perhaps of the type found in skeletal muscle, and the second is voltage-activated Na^+ influx, which might affect Ca^{2+} stores. The importance of Na^+ in the physiology of these terminals has been demonstrated in earlier work (Stuenkel and Nordmann, 1993). To test these possibilities we compared syntilla rates at −80 mV and after depolarization to −40 mV, in the absence of Ca^{2+} but with Na^+ either present or absent. At −80 mV, the rates (syntillas per second per terminal) in the presence and absence of Na^+, respectively, were: 0.50 ± 0.07 ($N = 33$) versus 0.47 ± 0.08 ($N = 27$); at −40 mV, the rates were 0.80 ± 0.11 ($N = 11$) versus 0.90 ± 0.14 ($N = 11$). Hence, at each potential the rates were not significantly different in the presence and absence of Na^+. However, in the absence of both Na^+ and Ca^{2+} a global increase in $[Ca^{2+}]$ was not observed in any of the terminals, whereas it was found in 44% of the terminals when Na^+ was present. The resting level of total fluorescence at −80 mV was not different in the presence versus absence of Na^+ (2.7 ± 0.3 (arbitrary units; $N = 55$) versus 2.8 ± 0.2 ($N = 57$), respectively. In sum, at least part of the increase in syntilla frequency, and perhaps all of it, is found in the absence of external Na^+ and is therefore independent of Na^+ influx. In contrast, the increase in global $[Ca^{2+}]$ at −40 mV is dependent on the presence of extracellular Na^+ (see Discussion).

Depolarizations to levels more than or equal to −40 mV or prolonged application of caffeine cause a global increase in cytosolic $[Ca^{2+}]$ in the absence of Ca^{2+} influx

As mentioned in the previous section, in 44% of the terminals, depolarization from −80 to −40 mV caused an increase in global cytosolic $[Ca^{2+}]$ (Fig. 6*A*), and this increase was attenuated by ryanodine (Fig. 6*B*). When the depolarization caused an increase

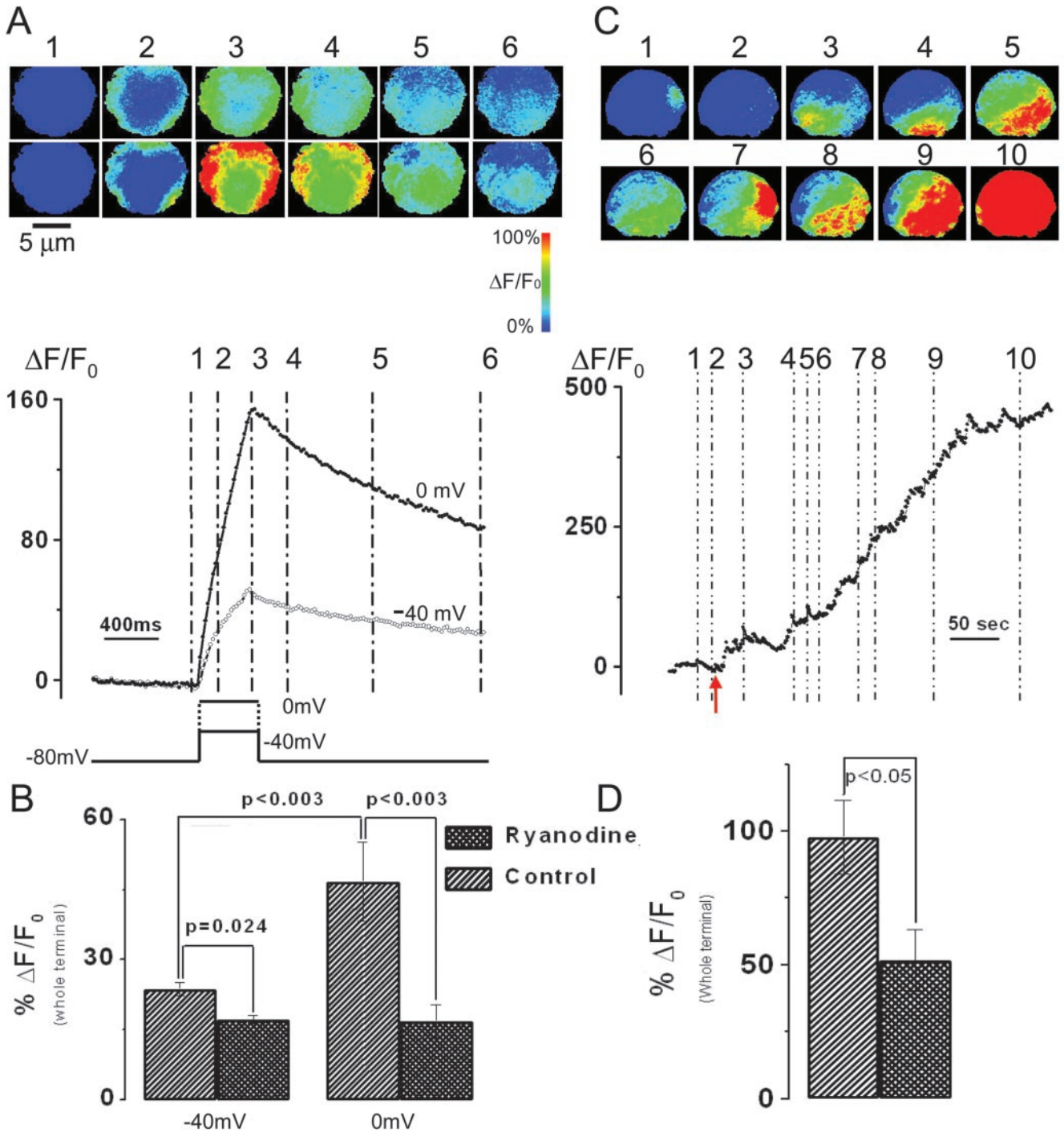

Figure 6. Stronger stimulation causes a rise in global $[Ca^{2+}]$ in absence of extracellular Ca^{2+}. *A,* Images showing increase in global $[Ca^{2+}]_i$ in same terminal after 400 msec depolarization to 0 mV (bottom row) or to −40 mV (top row), and traces showing time course of change in global $\Delta F/F_0$ corresponding to the images. *B,* Percentage change in global $\Delta F/F_0$ at end of 400 msec depolarization to −40 mV ($N = 23$) or 0 mV ($N = 22$) in the presence and absence of ryanodine ($N = 21$ and 23, respectively). *C,* Images showing increase in global $[Ca^{2+}]_i$ after 20 mM caffeine perfusion and traces showing time course of change in global $\Delta F/F_0$ corresponding to the images. Caffeine perfusion begins at red arrow and continues throughout. *D,* Percentage increase in global $\Delta F/F_0$ after 2 min of perfusion in the presence ($N = 3$) or absence ($N = 3$) of ryanodine. A total of 34 nerve terminals were used to acquire the data in the figure.

in global Ca^{2+}, one or several sites responded first with a local release of Ca^{2+} that was joined by other regions resulting in a rise in global $[Ca^{2+}]$ (Fig. 6*A*). In a given terminal the same site or sites were the first to respond after each of a series of successive depolarizations separated by a waiting interval. After depolarization from −80 to 0 mV, the increase in global cytosolic $[Ca^{2+}]$ was greater in magnitude than that at −40 mV, and it was attenuated by ryanodine (Fig. 6*A,B*). As with the global increase in $[Ca^{2+}]$ at −40 mV, the same focus or foci responded first during a series of successive depolarizations.

As described above, brief application of caffeine (4 sec, at −80 mV) from a puffer pipette located 50 μm from a terminal caused an increase in both syntilla frequency and the signal mass of individual syntillas, but not an increase in global $[Ca^{2+}]$. Longer application (1–5 min) by bath perfusion (20 mM caffeine) caused a global increase in $[Ca^{2+}]$, as illustrated in Figure 6*C*. As is

apparent in these images, individual localized events could be seen leading up to the global increase and within it. It is also clear from the images of Figure 6*C* that the global increase is not due to a wave-like spread from an initiation site or sites. As with the global increase induced by depolarization, the caffeine-induced global increase in $[Ca^{2+}]$ was attenuated by ryanodine (Fig. 6*D*).

Discussion

The regulation of Ca^{2+} syntillas by membrane potential

Ca^{2+} syntillas are unique in a variety of ways other than their origin in nerve terminals. The most striking of these distinctive features is the regulation of syntilla frequency by membrane potential in the absence of Ca^{2+} influx. Although CICR has often been suggested as a mechanism to cause Ca^{2+} release from ryanodine-sensitive Ca^{2+} stores in neurons, regulation of stores by membrane potential in the absence of Ca^{2+} influx has not been demonstrated in any neuronal structure or in any exocytotic cell type, to the best of our knowledge. The existence of voltage regulation in the nerve terminals studied here suggests that this mechanism may be present elsewhere in neurons. Regulation of miniature Ca^{2+} release events by membrane potential has been firmly established only in skeletal muscle fibers (Tsugorka et al., 1995), but the results of the present study suggest that an analogous mechanism may exist in nerve terminals. L-type Ca^{2+} channels have been identified in neurohypophysial terminals from the rat (Lemos and Nowycky, 1989), and these may possibly serve as a voltage sensor. This idea is supported by the finding of Chavis et al. (1996) in cerebellar granule cells that RyRs are tightly coupled to L-type Ca^{2+} channels and can enhance their activity. Alternatively the effect may be the result of an indirect coupling between L-type Ca^{2+} channels and RyRs of the type seen in smooth muscle, which is also independent of Ca^{2+} influx (del Valle-Rodriguez et al., 2003).

In the absence of both extracellular Na^+ and Ca^{2+}, depolarization from −80 to −40 mV elicited an increase in syntilla frequency so that voltage-activated Na^+ influx cannot account for the frequency increase. However, in the presence of extracellular Na^+, there was an additional effect of depolarization that led to a greater increase in global $[Ca^{2+}]$. This effect of external Na^+ reinforces the importance of Na^+ in the physiology of these terminals (Stuenkel and Nordmann, 1993; Turner and Stuenkel, 1998).

The spatiotemporal profile of Ca^{2+} syntillas

The ability of membrane potential in the absence of Ca^{2+} influx to increase syntilla firing rate suggests that the site of Ca^{2+} release in a syntilla resides quite close to the plasma membrane, a conclusion that is reinforced by maps of syntilla sites (Fig. 3*E*). Hence, we sought to determine the spatiotemporal profile of $[Ca^{2+}]$ caused by a syntilla in the region of the plasma membrane. To do so, we performed simulations to determine the spatiotemporal profile, as outlined in Materials and Methods, and the results are shown in Figure 7 with the input waveform shown in Figure 7*A*. The plots in Figure 7, *B* and *C*, present information in the same format as confocal line-scans, with time along the *x*-axis and distance along the *y*-axis and color providing the scale for concentration. Iso-concentration lines are used, as opposed to a continuous color depiction (as in line-scan images), because they make it possible to present a greater range of concentrations. Figure 7*B* shows the simulation of a syntilla directly under the PM. The green line is 10 μM (see legend), a concentration believed to be necessary for neuropeptide release (Lee et al., 1992). The 10 μM isoconcentration line reaches its maximum

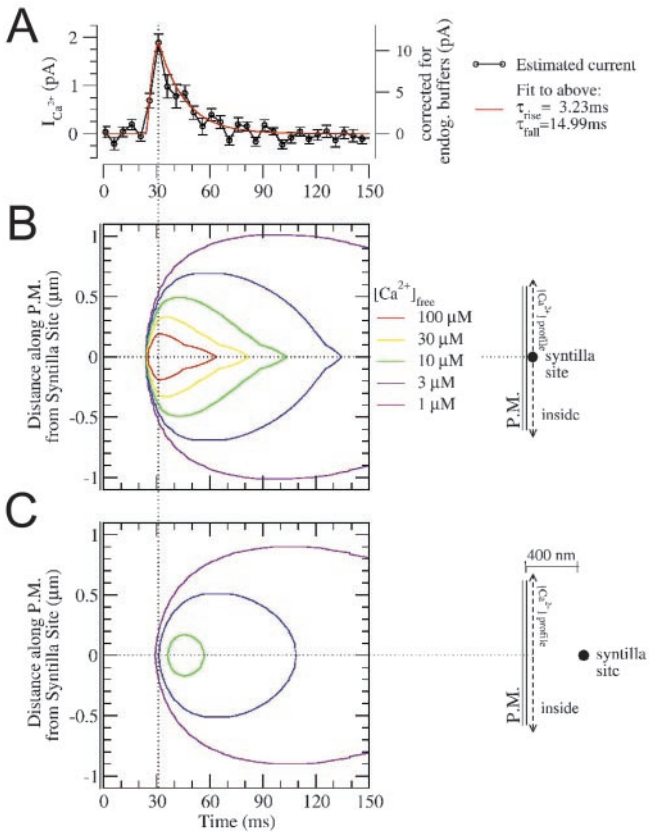

Figure 7. The spatiotemporal profile of $[Ca^{2+}]$ caused by a syntilla. *A,* The Ca^{2+} release current waveform for the simulated syntillas. The I_{Ca} waveform was taken from the experimentally determined Ca^{2+} current (see Results and Fig. 4*B*), shown in black circles and referred to the vertical scale on the left. To avoid the effect of noise in the estimated current, these data were fit with a function of two exponentials, one for the rising and one for the falling phases (red line, see legend for time constants, $R^2 = 0.92$). To take into account the additional Ca^{2+} taken up by the endogenous buffers, the amplitude of the Ca^{2+} current was multiplied by the relative buffering capacity) of the total endogenous buffer (see Materials and Methods), and this is reflected in the scale on the right. This fitted, scaled waveform (red line, right-side scale) was used as the syntilla I_{Ca} waveform in the simulations shown in *B* and *C*. The Ca^{2+} release was simulated over a period of 150 msec, with the peak of the release occurring at 31 msec. *B,* Simulation of a syntilla located directly under the plasma membrane. Isoconcentration lines show the values of free $[Ca^{2+}]$ taken along a line through the center of the release site. The vertical axis is distance along the PM away from the release site, and the horizontal axis is time. The observed 2-D symmetry along the vertical axis (distance from release) in fact occurs in 3-D, i.e., in all directions along the PM away from the release. *C,* Simulation of a syntilla located 400 nm away from the plasma membrane. In this case, the isoconcentration lines show the values of free $[Ca^{2+}]$ taken along a line directly.

spatial extent, a radius of ~500 nm, at ~10 msec after the peak of I_{Ca}. At a radius of 300 nm, $[Ca^{2+}]$ remains ≥10 μM for >40 msec. At distances >500 nm, the concentration will not reach 10 μM. Hence, it appears possible for a syntilla to activate proteins in its microdomain without triggering exocytosis at a site a few hundred nanometers away. This, in turn, means that the nerve terminal may be divided into more Ca^{2+} microdomains than those arising from Ca^{2+} influx alone. The same is true for syntilla sites not at the PM. For example, Figure 7*C* shows the simulation of a syntilla located 400 nm away from the PM. In this case, the isoconcentration lines show the values of free $[Ca^{2+}]$ taken along a line directly under the PM centered on the point on the PM closest to the release site. The $[Ca^{2+}]$ exceeds 10 μM within a radius of ~150 nm for 10–20 msec. When the site of release was moved farther away from the PM (i.e., 500 nm), the concentration at the PM did not reach 10 μM (data not shown).

The simulations demonstrate that syntillas are likely to result in supermicromolar concentrations over hundreds of nanometers for tens of milliseconds. Hence, syntillas may affect Ca^{2+} targets that are sensitive to supermicromolar concentrations of Ca^{2+} within a small region. A supermicromolar concentration of Ca^{2+} is necessary to affect some components of vesicle cycling (see below) (Sudhof and Rizo, 1996). Thus, it is possible for syntillas to affect targets of low Ca^{2+} sensitivity in the syntilla microdomain without acting on targets in different microdomains, perhaps, for example, microdomains inhabited by plasmalemmal Ca^{2+} channels where exocytosis is triggered.

The nature of the intraterminal stores providing Ca^{2+} for the syntillas

It is clear that neurohypophysial nerve terminals contain functional ryanodine receptors, as is evident from the sensitivity of syntillas to both caffeine and ryanodine. Because ryanodine affects both gating and conductance of RyRs in a concentration-dependent way, with an additional level of complexity added by the interaction of RyRs with one another and with other proteins in generating focal Ca^{2+} release, for example in striated muscle (Fill and Copello, 2002), it is not surprising that its action on syntillas is complicated. At a lower concentration (10 μM in the puffer pipette positioned 50 μm from the terminal; see Materials and Methods), ryanodine increased the syntilla frequency just as low concentrations increase the frequency of Ca^{2+} sparks in cardiac and skeletal muscle which are also mediated by RyRs (Satoh et al., 1998; Gonzalez et al., 2000; Hui et al., 2001). At this activating concentration of ryanodine, the amount of Ca^{2+} released per syntilla was decreased. This effect is reminiscent of the presence of low-amplitude focal Ca^{2+} transients in striated muscle at a concentration in which ryanodine increased spark frequency and is consistent with the induction by lower ryanodine concentrations of low conductance, high Po states of RyRs (Fill and Copello, 2002). At a higher concentration (100 μM in the bathing solution), ryanodine decreased the frequency of the syntillas, as might be expected since it blocks RyRs at higher concentrations (Fill and Copello, 2002). However, at this concentration ryanodine had no effect on the amount of Ca^{2+} released per syntilla, suggesting perhaps that syntilla sites were silenced by ryanodine after the generation of a syntilla, consistent with the use dependence of ryanodine action. Finally the ability of caffeine to increase the amount of Ca^{2+} released per syntilla could result from recruitment of more RyRs at a given release site or from an another effect of caffeine, for example an anti-phosphodiesterase action. The results with ryanodine and caffeine are supported by the immunocytochemical identification of RyRs whose distribution, like that of the syntillas, is not confined to one region of the terminal.

The failure of cyanide and azide to affect the syntillas suggests that mitochondria are not the source of the Ca^{2+} release reported here, although they may eventually turn out to provide some modulatory influences (Koizumi et al., 1999). One intriguing candidate for the source of syntilla Ca^{2+} is the neurosecretory granules in which preliminary studies using immunogold labeling have disclosed both RyRs and IP_3Rs (Salzberg et al., 2000). Moreover, in these neurosecretory granules, Ca^{2+} is stored at high levels that may be altered in the process of depolarization-induced secretion (Thirion et al., 1995). However, it is not clear how these results relate to our finding that TG, which is specific for SERCA pumps, drastically reduced the frequency of syntilla because SERCA pumps are generally considered to reside only on ER membrane. Hence, the possibility arises that more than one intracellular compartment may be involved in the generation of syntillas. Finally, the present study demonstrates that Ca^{2+} stores within nerve terminals must be considered as more than buffering mechanisms (Castonguay and Robitaille, 2001), because they can act to release Ca^{2+} in a quantal manner after physiological levels of depolarization.

The effect of Ca^{2+} syntillas on neurosecretion

It is well known that in nerve terminals extracellular Ca^{2+} provides the source that triggers neurotransmitter release. How then might Ca^{2+} from internal stores act to affect the secretion of neuropeptide in the terminals used here? The neurohypophysial nerve terminals possess at least two functionally distinct acutely releasable secretory granule pools that differ in size, rate, and Ca^{2+} sensitivity of exocytosis (Giovannucci and Stuenkel, 1997). The "immediately releasable pool" is characterized by an immediate jump in and rapid recovery of the resting membrane capacitance, and the "readily releasable pool" is typified by a slower membrane capacitance rise that persists after the stimulus. Giovanucci and Stuenkel (1997) suggested that the activation of unknown Ca^{2+}-dependent steps prepare the granules of the ready releasable pool for secretion. Indeed, in the trafficking route of recycling vesicles it is not well understood how vesicles that are not competent for release are freed from their restraints and how they travel to the membrane (Betz and Angleson, 1998). In this context several possibilities exist for the function of syntillas. First, it has been suggested that if motors are involved in vesicle mobilization, they must be activated selectively by nerve stimulation (Betz and Angleson, 1998; Ryan, 1999). Syntillas might provide the link between depolarization and motor driven vesicle mobilization. Second, *in vitro* studies have shown that phosphorylation by Ca^{2+} calmodulin kinase II of synapsin I reduces its affinity for the synaptic vesicle (De Camilli et al., 1990), and syntillas might provide the Ca^{2+} to elicit this phosphorylation and release the vesicle from the restraint imposed by synapsin I. In summary, Ca^{2+} is thought to have effects on many stages of the synaptic cycle (Sudhof and Rizo, 1996), including the processes by which vesicles are maintained in clusters, mobilized, and recruited for fusion with the plasma membrane, and the Ca^{2+} provided by syntillas may act on one or more of these processes to alter the level of neurosecretion.

References

Becker PL, Singer JJ, Walsh JVJ, Fay FS (1989) Regulation of calcium concentration in voltage-clamped smooth muscle cells. Science 244:211–214.

Berridge MJ (1998) Neuronal calcium signaling. Neuron 21:13–26.

Bers DM (2002) Cardiac excitation-contraction coupling. Nature 415:198–205.

Betz WJ, Angleson JK (1998) The synaptic vesicle cycle. Annu Rev Physiol 60:347–363.

Burbach JP, Luckman SM, Murphy D, Gainer H (2001) Gene regulation in the magnocellular hypothalamo-neurohypophysial system. Physiol Rev 81:1197–1267.

Cannell MB, Cheng H, Lederer WJ (1995) The control of calcium release in heart muscle. Science 268:1045–1049.

Carrington WA, Lynch RM, Moore ED, Isenberg G, Fogarty KE, Fay FS (1995) Superresolution three-dimensional images of fluorescence in cells with minimal light exposure. Science 268:1483–1487.

Carter AG, Vogt KE, Foster KA, Regehr WG (2002) Assessing the role of calcium-induced calcium release in short-term presynaptic plasticity at excitatory central synapses. J Neurosci 22:21–28.

Castonguay A, Robitaille R (2001) Differential regulation of transmitter release by presynaptic and glial Ca^{2+} internal stores at the neuromuscular synapse. J Neurosci 21:1911–1922.

Chavis P, Fagni L, Lansman JB, Bockaert J (1996) Functional coupling be-

tween ryanodine receptors and L-type calcium channels in neurons. Nature 382:719–722.
Cheng H, Lederer WJ, Cannell MB (1993) Calcium sparks: elementary events underlying excitation-contraction coupling in heart muscle. Science 262:740–744.
De Camilli P, Benfenati F, Valtorta F, Greengard P (1990) The synapsins. Annu Rev Cell Biol 6:433–460.
De Crescenzo V, Zhuge R, Velázquez-Marrero C, Lifshitz LM, Custer E, Carmichael JD, Lai A, Tuft R, Fogarty KE, Lémos JR, Walsh JV (2003) Miniature Ca^{2+} release events (Ca^{2+} syntillas) in nerve terminals are increased in frequency by depolarization. Biophys J 84:1886.
del Valle-Rodriguez A, Lopez-Barneo J, Urena J (2003) Ca2+ channel-sarcoplasmic reticulum coupling: a mechanism of arterial myocyte contraction without Ca^{2+} influx. EMBO J 22:4337–4345.
Drummond RM, Mix TC, Tuft RA, Walsh Jr JV, Fay FS (2000) Mitochondrial Ca^{2+} homeostasis during Ca^{2+} influx and Ca^{2+} release in gastric myocytes from *Bufo marinus*. J Physiol (Lond) 522:375–390.
Ehrlich BE, Kaftan E, Bezprozvannaya S, Bezprozvanny I (1994) The pharmacology of intracellular Ca^{2+}-release channels. Trends Pharmacol Sci 15:145–149.
Emptage NJ, Reid CA, Fine A (2001) Calcium stores in hippocampal synaptic boutons mediate short-term plasticity, store-operated Ca^{2+} entry, and spontaneous transmitter release. Neuron 29:197–208.
Fill M, Copello JA (2002) Ryanodine receptor calcium release channels. Physiol Rev 82:893–922.
Giovannucci DR, Stuenkel EL (1997) Regulation of secretory granule recruitment and exocytosis at rat neurohypophysial nerve endings. J Physiol (Lond) 498:735–751.
Gonzalez A, Kirsch WG, Shirokova N, Pizarro G, Brum G, Pessah IN, Stern MD, Cheng H, Rios E (2000) Involvement of multiple intracellular release channels in calcium sparks of skeletal muscle. Proc Natl Acad Sci USA 97:4380–4385.
Grynkiewicz G, Poenie M, Tsien RY (1985) A new generation of Ca^{2+} indicators with greatly improved fluorescence properties. J Biol Chem 260:3440–3450.
Hui CS, Bidasee KR, Besch HRJ (2001) Effects of ryanodine on calcium sparks in cut twitch fibres of *Rana temporaria*. J Physiol (Lond) 534:327–342.
Kargacin G, Fay FS (1991) Ca^{2+} movement in smooth muscle cells studied with one- and two-dimensional diffusion models. Biophys J 60:1088–1100.
Klingauf J, Neher E (1997) Modeling buffered Ca^{2+} diffusion near the membrane: implications for secretion in neuroendocrine cells. Biophys J 72:674–690.
Koizumi S, Bootman MD, Bobanovic LK, Schell MJ, Berridge MJ, Lipp P (1999) Characterization of elementary Ca^{2+} release signals in NGF- differentiated PC12 cells and hippocampal neurons. Neuron 22:125–137.
Krizaj D, Bao JX, Schmitz Y, Witkovsky P, Copenhagen DR (1999) Caffeine-sensitive calcium stores regulate synaptic transmission from retinal rod photoreceptors. J Neurosci 19:7249–7261.
Lee CJ, Dayanithi G, Nordmann JJ, Lemos JR (1992) Possible role during exocytosis of a Ca^{2+}-activated channel in neurohypophysial granules. Neuron 8:335–342.
Lemos JR, Nowycky MC (1989) Two types of calcium channels coexist in peptide-releasing vertebrate nerve terminals. Neuron 2:1419–1426.
Llano I, Gonzalez J, Caputo C, Lai FA, Blayney LM, Tan YP, Marty A (2000) Presynaptic calcium stores underlie large-amplitude miniature IPSCs and spontaneous calcium transients. Nat Neurosci 3:1256–1265.
Mejia-Alvarez R, Kettlun C, Rios E, Stern M, Fill M (1999) Unitary Ca^{2+} current through cardiac ryanodine receptor channels under quasi-physiological ionic conditions. J Gen Physiol 113:177–186.
Melamed-Book N, Kachalsky SG, Kaiserman I, Rahamimoff R (1999) Neuronal calcium sparks and intracellular calcium "noise". Proc Natl Acad Sci USA 96:15217–15221.
Meldolesi J (2001) Rapidly exchanging Ca^{2+} stores in neurons: molecular, structural and functional properties. Prog Neurobiol 65:309–338.
Naraghi M, Neher E (1997) Linearized buffered Ca^{2+} diffusion in microdomains and its implications for calculation of $[Ca^{2+}]$ at the mouth of a calcium channel. J Neurosci 17:6961–6973.
Narita K, Akita T, Osanai M, Shirasaki T, Kijima H, Kuba K (1998) A Ca^{2+}-induced Ca^{2+} release mechanism involved in asynchronous exocytosis at frog motor nerve terminals. J Gen Physiol 112:593–609.
Neher E (1998) Vesicle pools and Ca^{2+} microdomains: new tools for understanding their roles in neurotransmitter release. Neuron 20:389–399.
Nordmann JJ, Dayanithi G, Lemos JR (1987) Isolated neurosecretory nerve endings as a tool for studying the mechanism of stimulus-secretion coupling. Biosci Rep 7:411–425.
O'Reilly CM, Fogarty KE, Drummond RM, Tuft RA, Walsh JVJ (2003) Quantitative analysis of spontaneous mitochondrial depolarizations. Biophys J 85:3350–3357.
Parker I, Yao Y (1991) Regenerative release of calcium from functionally discrete subcellular stores by inositol trisphosphate. Proc R Soc Lond B Biol Sci 246:269–274.
Ryan TA (1999) Inhibitors of myosin light chain kinase block synaptic vesicle pool mobilization during action potential firing. J Neurosci 19:1317–1323.
Salzberg BM, Muschol M, Kraner SD, Obaid AL (2000) Localization of calcium release channels to secretory granules in terminals of the mouse neurohypophysis. Biophys J 78: 260A.
Satoh H, Katoh H, Velez P, Fill M, Bers DM (1998) Bay K 8644 increases resting Ca^{2+} spark frequency in ferret ventricular myocytes independent of Ca influx: contrast with caffeine and ryanodine effects. Circ Res 83:1192–1204.
Smith GD, Keizer JE, Stern MD, Lederer WJ, Cheng H (1998) A simple numerical model of calcium spark formation and detection in cardiac myocytes. Biophys J 75:15–32.
Stuenkel EL (1994) Regulation of intracellular calcium and calcium buffering properties of rat isolated neurohypophysial nerve endings. J Physiol (Lond) 481:251–271.
Stuenkel EL, Nordmann JJ (1993) Sodium-evoked, calcium-independent vasopressin release from rat isolated neurohypophysial nerve endings. J Physiol (Lond) 468:357–378.
Sudhof TC, Rizo J (1996) Synaptotagmins: C2-domain proteins that regulate membrane traffic. Neuron 17:379–388.
Sun XP, Callamaras N, Marchant JS, Parker I (1998) A continuum of InsP3-mediated elementary Ca^{2+} signalling events in *Xenopus* oocytes. J Physiol (Lond) 509:67–80.
Thirion S, Stuenkel EL, Nicaise G (1995) Calcium loading of secretory granules in stimulated neurohypophysial nerve endings. Neuroscience 64:125–137.
Troadec JD, Thirion S, Nicaise G, Lemos JR, Dayanithi G (1998) ATP-evoked increases in [Ca2+]i and peptide release from rat isolated neurohypophysial terminals via a P2X2 purinoceptor. J Physiol (Lond) 511:89–103.
Tsugorka A, Rios E, Blatter LA (1995) Imaging elementary events of calcium release in skeletal muscle cells. Science 269:1723–1726.
Tunwell RE, Wickenden C, Bertrand BM, Shevchenko VI, Walsh MB, Allen PD, Lai FA (1996) The human cardiac muscle ryanodine receptor-calcium release channel: identification, primary structure and topological analysis. Biochem J 318:477–487.
Turner D, Stuenkel EL (1998) Effects of depolarization evoked Na+ influx on intracellular Na+ concentration at neurosecretory nerve endings. Neuroscience 86:547–556.
Wang XM, Treistman SN, Wilson A, Nordmann JJ, Lemos JR (1993) Ca^{2+} channels and peptide release from neurosecretory terminals. News Physiol Sci 8:64–68.
Zhou Z, Neher E (1993) Mobile and immobile calcium buffers in bovine adrenal chromaffin cells. J Physiol (Lond) 469:245–273.
ZhuGe R, Fogarty KE, Tuft RA, Lifshitz LM, Sayar K, Walsh JV Jr (2000) Dynamics of signaling between Ca(2+) sparks and Ca(2+)- activated K(+) channels studied with a novel image-based method for direct intracellular measurement of ryanodine receptor Ca(2+) current. J Gen Physiol 116:845–864.
ZhuGe R, Fogarty KE, Tuft RA, Walsh JV Jr (2002) Spontaneous transient outward currents arise from microdomains where BK channels are exposed to a mean Ca(2+) concentration on the order of 10 micromolar during a Ca(2+) spark. J Gen Physiol 120:15–28.
ZhuGe R, Tuft RA, Fogarty KE, Bellve K, Fay FS, Walsh JV Jr (1999) The influence of sarcoplasmic reticulum Ca^{2+} concentration on Ca^{2+} sparks and spontaneous transient outward currents in single smooth muscle cells. J Gen Physiol 113:215–228.